ANALYSES OF DELAMINATIONS IN NON-LINEAR ELASTIC MULTILAYERED INHOMOGENEOUS BEAM CONFIGURATIONS

Victor Rizov*

Department of Technical Mechanics, Faculty of Hydro-technique, University of Architecture, Civil Engineering and Geodesy, 1 Chr. Smirnesky blvd., 1046 - Sofia, Bulgaria

ARTICLE INFO

***Article history*:**
Received: 11.7.2018.
Received in revised form: 8.11.2018.
Accepted: 22.11.2018.

Keywords:
Inhomogeneous material
Delamination
Material non-linearity
J-integral
Strain energy release rate
Four-point bending
Multilayered beam
Complementary strain energy

DOI: http://doi.org/10.30765/er.40.3.07

Abstract:

This paper presents investigation of delamination fracture behavior of multilayered non-linear elastic beam configurations by using the Ramberg-Osgood stress-strain relation. It is assumed that each layer exhibits continuous material inhomogeneity along the width as well as along thickness of the layer. An approach for determination of the strain energy release rate is developed for a delamination crack located arbitrary along the multilayered beam height. The approach can be applied for multilayered beams of arbitrary cross-section under combination of axial force and bending moments. The layers may have different thickness and material properties. The number of layers is arbitrary. The approach is applied for analyzing the delamination fracture behavior of a multilayered beam configuration subjected to four-point bending. The beam has a rectangular cross-section. The delamination crack is located symmetrically with respect to the beam mid-span. The strain energy release rate is derived assuming that the modulus of elasticity varies continuously in the cross-section of each layer according to a hyperbolic law. In order to verify the solution to the strain energy release rate, the delamination fracture behavior of the multilayered non-linear elastic four-point bending beam configuration is studied also by applying the method of the J-integral. The solution to the strain energy release rate derived in the present paper is used in order to perform a parametric study of delamination.

* Corresponding author. Tel.: + (359-2) 963 52 45 / 664; fax: + (359-2) 86 56 863
E-mail address: v_rizov_fhe@uacg.bg

1 Introduction

Inhomogeneous structural materials exhibit varying material properties in the volume of the solid. Since the material properties are functions of the coordinates, the analysis of fracture in structural members and components made of inhomogeneous materials is a challenging problem. Nevertheless, the development of fracture analyses is an important task of the fracture mechanics of inhomogeneous materials because these analyses give useful information about the influence of various factors such as geometry of the structural member, crack location, material response and others on the fracture behaviour. This information can be significant in order to better understand the fracture phenomenon. Also, the knowledge gathered through these analyses can be used in the design of inhomogeneous structural components in order to improve and optimize their fracture performance.

One of the reasons for the increased interest towards the inhomogeneous materials is that the functionally graded materials, which are a class of inhomogeneous materials, have been widely applied in practical engineering [1-12]. Functionally graded materials are made by mixing two or more constituent materials. Due to the variation of material properties along one or more spatial coordinates, the microstructure of functionally graded materials can be tailored during manufacturing. This fact makes these new inhomogeneous materials an attractive alternative to the conventional structural materials in various applications in aerospace systems, aircrafts, nuclear power plants, microelectronics and biomedicine.

Multilayered materials are a kind of inhomogeneous materials which are made of adhesively bonded layers of different materials. The concept of multilayered materials opens excellent opportunities for adequate utilization of strength of different materials assembled in one structure and provides an effective mean for optimization of structural performance. Thus, the multilayered structures have a high load-bearing capacity and are usually much more economical in comparison with their metal counterparts. Since the stiffness-to-weight and strength-to-weight ratios of multilayered materials are high, significant weight savings can be realized. Therefore, multilayered materials are very suitable for light structures in various engineering applications where low weight is particularly important.

One of the major concerns in the use of multilayered materials and structures in practical engineering is their delamination fracture behaviour. The delamination phenomenon involves longitudinal fracture, i.e. separation of adjacent layers. In fact, the delamination is the most often type of failure occurring in multilayered structures. The safety and durability of multilayered structural members and components depend strongly upon their delamination behaviour. Usually, fracture in multilayered structural components has been studied by the methods of linear-elastic fracture mechanics assuming linear-elastic behaviour of the material [13, 14].

Recently, particular delamination fracture analyses of non-linear elastic multilayered beam configurations of rectangular cross-section loaded in bending have been developed assuming that each layer exhibits material inhomogeneity [15-17]. The material non-linearity has been modeled mainly by using power-law stress-strain relations.

The delamination fracture behaviour of a non-linear elastic multilayered beam structure of rectangular cross-section has been studied in terms of the strain energy release rate [17]. The beam is made of vertical longitudinal adhesively bonded layers. A delamination crack is located arbitrary between layers. It has been assumed that the layers exhibit material inhomogeneity in the thickness direction. The beam is loaded in bending about the horizontal centroidal axis of the cross-section. The non-linear mechanical behaviour of the material has been treated by using a power-law stress-strain relation. A solution to the strain energy release rate has been derived assuming that the coefficient in the power-law varies continuously along the thickness of layers.

This paper presents a general approach for determination of the strain energy release rate for delamination cracks in multilayered non-linear elastic beams is developed by using the Ramberg-Osgood stress-strain relationship for modeling the material non-linearity in contrast to previous papers [15-17] which are concerned with particular solutions of the strain energy release rate for separate beam configurations. Multilayered beams of arbitrary cross-section are considered in the present paper. The beams are made of arbitrary number of adhesively bonded horizontal layers. Each layer has individual thickness and material properties. Besides, it is assumed that each layer exhibits smooth material inhomogeneity along the width as well as along thickness of layer. The delamination crack is located arbitrary between layers. The beams considered are

under combination of axial force and bending moments. The approach developed in the present paper is applied for studying the strain energy release rate for a delamination crack in a multilayered non-linear elastic inhomogeneous beam configuration subjected to four-point bending. The method of *J*-integral is used also for analysis of the delamination fracture behaviour of the multilayered four-point bending beam in order to verify the solution to the strain energy release rate.

2 Approach for determination of the strain energy release rate

A beam portion with the delamination crack front is shown schematically in Fig. 1.

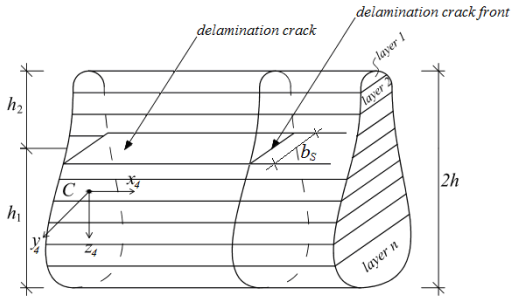

Figure 1. Portion of a multilayered beam with the delamination crack front (b_S is the beam width at the delamination crack level)

The heights of the lower and upper crack arms are denoted by h_1 and h_2, respectively. The non-linear mechanical behaviour of the inhomogeneous material in the *i*-th layer of the beam is described by the Ramberg-Osgood stress-strain relationship

$$\varepsilon = \frac{\sigma_i}{E_i} + \left(\frac{\sigma_i}{H_i}\right)^{\frac{1}{m_i}}, i = 1, 2, ..., n \tag{1}$$

where n is the number of layers in the beam, ε is the longitudinal strain, σ_i is the longitudinal normal stresses, E_i is the modulus of elasticity, H_i and m_i are material properties in the *i*-th layer. It is assumed that the modulus of elasticity varies continuously in the cross-section of each layer

$$E_i = E_i(y_4, z_4),\ i = 1, 2, ..., n \tag{2}$$

where y_4 and z_4 are the centroidal axes of the beam cross-section (Fig. 1).

The delamination fracture behaviour is analyzed in terms of the strain energy release rate, G. By applying the solution to the strain energy release rate derived in [18], the strain energy release rate for the multilayered beam in Fig. 1 can be written as

$$G = \frac{1}{b_S}\left(\begin{array}{l}\sum\limits_{i=1}^{i=n_1}\ \iint\limits_{(A)} u_{01i}^{*}\,dA + \\ \sum\limits_{i=1}^{i=n_2}\ \iint\limits_{(A)} u_{02i}^{*}\,dA - \sum\limits_{i=1}^{n}\ \iint\limits_{(A)} u_{0i}^{*}\,dA\end{array}\right) \tag{3}$$

where b_S is the beam width at the level of the delamination crack, n_1 and n_2 are, respectively, the number of layers in the lower and upper crack arms, u_{01i}^{*}, u_{02i}^{*} and u_{0i}^{*} are, respectively, the complementary strain energy densities in the *i*-th layer in the cross-section of the lower and upper crack arms behind the crack front and in the beam cross-section ahead of the crack front.

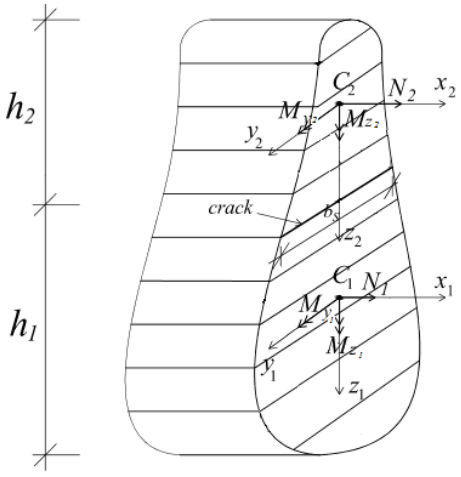

Figure 2. Cross-section of the lower and upper crack arms behind the crack front

The complementary strain energy density in the *i*-th layer of the cross-section of lower crack arm behind the crack front can be calculated by the following formula [19]:

$$u_{01i}^{*} = \frac{\sigma_i^2}{2E_i} + \frac{m_i \sigma_i^{\frac{1+m_i}{m_i}}}{(1+m_i)H^{\frac{1}{m_i}}} \tag{4}$$

In order to perform the integration of u_{01i}^{*} in (3), u_{01i}^{*} in (4) has to be expressed as a function of the coordinates, y_1 and z_1, (Fig. 2). Apparently, the normal stress, σ_i, cannot be determined explicitly from the equation of Ramberg-Osgood (1). Therefore, σ_i is expanded in series of Taylor by keeping the first six members

$$\begin{aligned}\sigma_i(y_1,z_1) \approx \sigma_i(0,z_{1ai}) + \frac{\partial \sigma_i(0,z_{1ai})}{\partial y_1} y_1 \\ + \frac{\partial \sigma_i(0,z_{1ai})}{\partial z_1}(z_1 - z_{1ai}) + \frac{\partial^2 \sigma_i(0,z_{1ai})}{2!\partial y_1^2} y_1^2 \\ + \frac{\partial^2 \sigma_i(0,z_{1ai})}{\partial y_1 \partial z_1} y_1 (z_1 - z_{1ai}) + \\ + \frac{\partial^2 \sigma_i(0,z_{1ai})}{2!\partial z_1^2}(z_1 - z_{1ai})^2\end{aligned} \tag{5}$$

where y_1 and z_1 are the centroidal axes of the lower crack arm cross-section (Fig. 2). In (5),

$$z_{1ai} = \frac{z_{1i} + z_{1i+1}}{2} \tag{6}$$

where z_{1i} and z_{1i+1} are the z_1-coordinates, respectively, of the upper and lower surfaces of the *i*-th layer.

Formula (5) is re-written as

$$\begin{aligned}\sigma_i(y_1,z_1) \approx \nu_{1i} + \nu_{2i} y_1 + \nu_{3i}(z_1 - z_{1ai}) \\ + \nu_{4i} y_1^2 + \nu_{5i} y_1 (z_1 - z_{1ai}) + \nu_{6i}(z_1 - z_{1ai})^2\end{aligned} \tag{7}$$

where the coefficients, ν_{1i}, ν_{2i}, ν_{3i}, ν_{4i}, ν_{5i} and ν_{6i}, are determined by applying the Ramberg-Osgood equation (1). For this purpose, by using the Bernoulli's hypothesis for plane sections, the strains in the lower crack arm cross-section are written as

$$\varepsilon = \varepsilon_{C_1} + \kappa_{y_1} y_1 + \kappa_{z_1} z_1 \tag{8}$$

where ε_{C_1} is the strain in the centre of the lower crack arm cross-section, κ_{y_1} and κ_{z_1} are the curvatures of lower crack arm in the x_1y_1 and x_1z_1 planes, respectively. The applicability of the Bernoulli's hypothesis is based on the fact that beams of high span to height ratio are analyzed in the present study. By substituting of (7) and (8) in (1), one obtains

$$\begin{aligned}\varepsilon_{C_1} + \kappa_{y_1} y_1 + \kappa_{z_1} z_1 = \\ \frac{1}{E_i}\left[\nu_{1i} + \nu_{2i} y_1 + \nu_{3i}(z_1 - z_{1ai}) + \nu_{4i} y_1^2 + \right. \\ \left. \nu_{5i} y_1 (z_1 - z_{1ai}) + \nu_{6i}(z_1 - z_{1ai})^2\right] + \\ + \frac{1}{H_i^{\frac{1}{m_i}}}\left[\nu_{1i} + \nu_{2i} y_1 + \nu_{3i}(z_1 - z_{1ai}) + \nu_{4i} y_1^2 + \right. \\ \left. + \nu_{5i} y_1 (z_1 - z_{1ai}) + \nu_{6i}(z_1 - z_{1ai})^2\right]^{\frac{1}{m_i}}\end{aligned} \tag{9}$$

At $y_1 = 0$ and $z_1 = z_{1ai}$, formula (9) transforms in

$$\varepsilon_{C_1} + \kappa_{Z_1} z_{1ai} = \frac{\nu_{1i}}{E_i} + \frac{\nu_{1i}^{\frac{1}{m_i}}}{H_i^{\frac{1}{m_i}}} \tag{10}$$

By substituting of $y_1 = 0$ and $z_1 = z_{1ai}$ in the first derivatives of (9) with respect to y_1 and z_1, one arrives at

$$\begin{aligned}\kappa_{y_1} E_i + \varepsilon_{C_1} \frac{\partial E_i}{\partial y_1} = \nu_{2i} + \\ + \frac{1}{H_i^{\frac{1}{m_i}}}\left(\frac{\partial E_i}{\partial y_1} \nu_{1i}^{\frac{1}{m_i}} + E_i \frac{1}{m_i} \nu_{1i}^{\frac{1-m_i}{m_i}} \nu_{2i}\right)\end{aligned} \tag{11}$$

$$\begin{aligned}\kappa_{z_1} E_i + \varepsilon_{C_1} \frac{\partial E_i}{\partial z_1} = \nu_{3i} + \\ + \frac{1}{H_i^{\frac{1}{m_i}}}\left(\frac{\partial E_i}{\partial z_1} \nu_{1i}^{\frac{1}{m_i}} + E_i \frac{1}{m_i} \nu_{1i}^{\frac{1-m_i}{m_i}} \nu_{3i}\right)\end{aligned} \tag{12}$$

Further, by substituting of $y_1 = 0$ and $z_1 = z_{1ai}$ in the second derivatives of (9) with respect to y_1 and z_1 one obtains

$$2\kappa_{y_1}\frac{\partial E_i}{\partial y_1}+\varepsilon_{C_1}\frac{\partial^2 E_i}{\partial y_1^2}=2\nu_{4i}+\frac{1}{H_i^{\frac{1}{m_i}}}\left[\frac{\partial^2 E_i}{\partial y_1^2}\nu_{1i}^{\frac{1}{m_i}}+\frac{\partial E_i}{\partial y_1}\frac{1}{m_i}\nu_{1i}^{\frac{1-m_i}{m_i}}\nu_{2i}+\left(\frac{\partial E_i}{\partial y_1}\frac{1}{m_i}\nu_{1i}^{\frac{1-m_i}{m_i}}+E_i\frac{1-m_i}{m_i^2}\nu_{1i}^{\frac{1-2m_i}{m_i}}\nu_{2i}\right)\nu_{2i}+E_i\frac{2}{m_i}\nu_{i1}^{\frac{1-m_i}{m_i}}\nu_{4i}\right] \tag{13}$$

$$\kappa_{y_1}\frac{\partial E_i}{\partial z_1}+\kappa_{z_1}\frac{\partial E_i}{\partial y_1}+\varepsilon_{C_1}\frac{\partial^2 E_i}{\partial y_1\partial z_1}=\nu_{5i}+\frac{1}{H_i^{\frac{1}{m_i}}}\left[\frac{\partial^2 E_i}{\partial y_1\partial z_1}\nu_{1i}^{\frac{1}{m_i}}+\frac{\partial E_i}{\partial y_1}\frac{1}{m_i}\nu_{1i}^{\frac{1-m_i}{m_i}}\nu_{3i}+\left(\frac{\partial E_i}{\partial z_1}\frac{1}{m_i}\nu_{i1}^{\frac{1-m_i}{m_i}}+E_i\frac{1-m_i}{m_i^2}\nu_{1i}^{\frac{1-2m_i}{m_i}}\nu_{3i}\right)\nu_{2i}+E_i\frac{1}{m_i}\nu_{1i}^{\frac{1-m_i}{m_i}}\nu_{5i}\right] \tag{14}$$

$$2\kappa_{z_1}\frac{\partial E_i}{\partial z_1}+\varepsilon_{C_1}\frac{\partial^2 E_i}{\partial z_1^2}=2\nu_{6i}+\frac{1}{H_i^{\frac{1}{m_i}}}\left[\frac{\partial^2 E_i}{\partial z_1^2}\nu_{1i}^{\frac{1}{m_i}}+\frac{\partial E_i}{\partial z_1}\frac{1}{m_i}\nu_{1i}^{\frac{1-m_i}{m_i}}\nu_{3i}+\left(\frac{\partial E_i}{\partial z_1}\frac{1}{m_i}\nu_{1i}^{\frac{1-m_i}{m_i}}+E_i\frac{1-m_i}{m_i^2}\nu_{1i}^{\frac{1-2m_i}{m_i}}\nu_{3i}\right)\nu_{3i}+E_i\frac{2}{m_i}\nu_{1i}^{\frac{1-m_i}{m_i}}\nu_{6i}\right] \tag{15}$$

It should be specified that the modulus of elasticity and its derivatives, $\frac{\partial E_i}{\partial y_1}$, $\frac{\partial E_i}{\partial z_1}$, $\frac{\partial^2 E_i}{\partial y_1^2}$, $\frac{\partial^2 E_i}{\partial y_1\partial z_1}$ and $\frac{\partial^2 E_i}{\partial z_1^2}$, which participate in equations (10) – (15) have to be calculated at $y_1=0$ and $z_1=z_{1ai}$.

Equations (10) – (15) can be written for each layer in the lower crack arm. In this way, $6n_1$ equations with $6n_1+3$ unknowns, ε_{C_1}, κ_{y_1}, κ_{z_1} and ν_{1i}, ν_{2i}, ν_{3i}, ν_{4i}, ν_{5i}, ν_{6i} where $i=1,2,...,n_1$, can be obtained. Three other equations can be written by considering the equilibrium of the lower crack arm cross-section which is under combination of axial force and bending moments (Fig. 2). The equilibrium equations are expressed as

$$N_1=\sum_{i=1}^{i=n_1}\iint_{(A)}\sigma_i dA \tag{16}$$

$$M_{y_1}=\sum_{i=1}^{i=n_1}\iint_{(A)}\sigma_i z_1 dA \tag{17}$$

$$M_{z_1}=\sum_{i=1}^{i=n_1}\iint_{(A)}\sigma_i y_1 dA \tag{18}$$

where σ_i is found by (7). In (16) – (18), N_1 is the axial force, M_{y_1} and M_{z_1} are the bending moments about the centroidal axes, y_1 and z_1. Equations (10) – (18) should be solved with respect to ε_{C_1}, κ_{y_1}, κ_{z_1}, ν_{1i}, ν_{2i}, ν_{3i}, ν_{4i}, ν_{5i} and ν_{6i} where $i=1,2,...,n_1$, by using the MATLAB R2013a computer program for particular beam structure and material properties. Then, u_{01i}^{*} where $i=1,2,...,n_1$ can be obtained by substituting (7) in (4).

The complementary strain energy density in the *i*-th layer of upper crack arm behind the crack front can be calculated using formula (4). For this purpose, σ_i has to be replaced with σ_{gi} where σ_{gi} is the normal stress in the *i*-th layer of upper crack arm. Besides, ε_{C_1}, κ_{y_1}, κ_{z_1}, ν_{1i}, ν_{2i}, ν_{3i}, ν_{4i}, ν_{5i}, ν_{6i}, n_1, N_1, M_{y_1} and M_{z_1} have to be replaced, respectively, with ε_{C_2}, κ_{y_2}, κ_{z_2}, ν_{g1i}, ν_{g2i}, ν_{g3i}, ν_{g4i}, ν_{g5i}, ν_{g6i}, n_2, N_2, M_{y_2} and M_{z_2} in equations (10) – (18). Here, ε_{C_2}, κ_{y_2} and κ_{z_2} are, respectively, the strain in the centre of the upper crack arm cross-section, and the curvatures in the x_2y_2 and x_2z_2 planes, N_2, M_{y_2} and M_{z_2} are the axial force and the bending moments (Fig. 2). After solving

equations (10) – (18) with respect to ε_{C_2}, κ_{y_2}, κ_{z_2}, ν_{g1i}, ν_{g2i}, ν_{g3i}, ν_{g4i}, ν_{g5i} and ν_{g6i}, the normal stress, σ_{gi}, can be expressed by (7) and then substituted in (4).

Formula (4) can also be applied to calculate u_{0i}^{*} by replacing of σ_i with σ_{ri}. The normal stress, σ_{ri}, in the *i*-th layer of the beam cross-section ahead of the crack front can be expressed by replacing of ν_{1i}, ν_{2i}, ν_{3i}, ν_{4i}, ν_{5i}, ν_{6i}, z_{1ai}, y_1 and z_1, respectively, with ν_{r1i}, ν_{r2i}, ν_{r3i}, ν_{r4i}, ν_{r5i}, ν_{r6i}, z_{3ai}, y_3 and z_3 in (7). Here, y_3 and z_3 are the centroidal axes of the beam cross-section ahead of the crack front (Fig. 3).

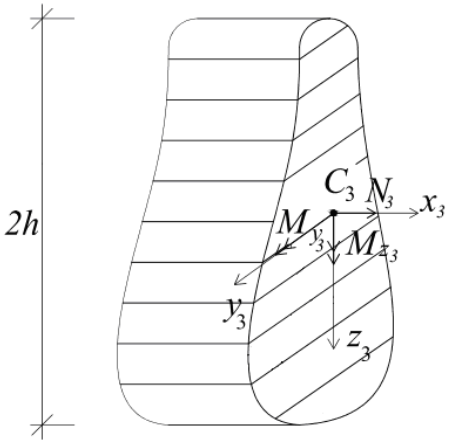

Figure 3. Beam cross-section ahead of the crack front

Also, ε_{C_1}, κ_{y_1}, κ_{z_1}, ν_{1i}, ν_{2i}, ν_{3i}, ν_{4i}, ν_{5i}, ν_{6i}, n_1, N_1, M_{y_1} and M_{z_1} are replaced, respectively, with ε_{C_3}, κ_{y_3}, κ_{z_3}, ν_{r1i}, ν_{r2i}, ν_{r3i}, ν_{r4i}, ν_{r5i}, ν_{r6i}, n, N_3, M_{y_3} and M_{z_3} in equations (10) – (18).

After substituting of u_{01i}^{*}, u_{02i}^{*} and u_{0i}^{*} in (3), the strain energy release rate can be calculated for given beam geometry, loading and material properties (the integration in (3) should be performed by using the MATLAB R2013a computer program).

3 Numerical results

In this section, numerical results are presented in order to illustrate the capabilities of the approach for determination of the strain energy release rate developed in section 2 of this paper. Delamination fracture behaviour of a multilayered inhomogeneous beam configuration of rectangular cross-section is investigated. The beam is shown schematically in Fig. 4.

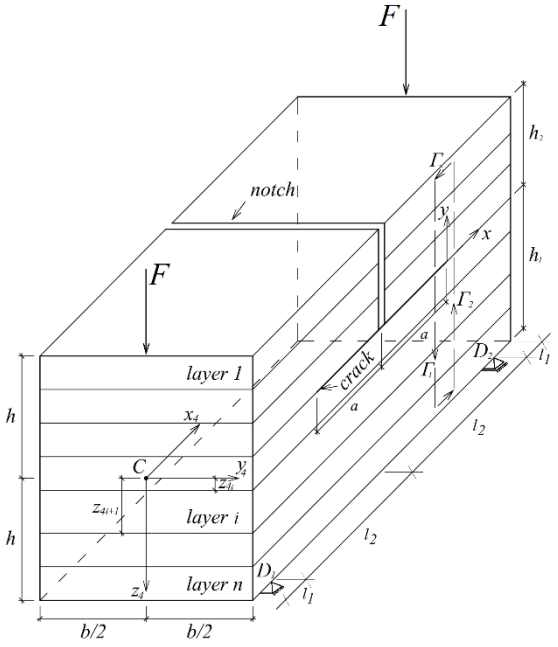

Figure 4. Four-point bending multilayered beam configuration

The cross-section of the beam has width, b, and height, $2h$. The beam is subjected to four-point bending. The external loading consists of two vertical forces, F, applied at the end sections of the beam. A vertical notch of depth h_2 is introduced under the upper beam surface in order to generate conditions for delamination fracture. It is assumed that a delamination crack of length $2a$ is located symmetrically with respect to the beam mid-span. The heights of the lower and upper crack arms are denoted by h_1 and h_2, respectively. It is obvious that the upper crack arm is free of stresses. The delamination crack is located in the middle beam portion, D_1D_2, that is loaded in pure bending. Due to the symmetry, only half of the beam, $l_1 + l_2 \le x_4 \le 2(l_1 + l_2)$, is analyzed (Fig. 4).

The delamination fracture is studied in terms of the strain energy release rate by using formula (3). For this purpose, first, the complementary strain energy density in the *i*-th layer of the lower crack arm behind the crack front is calculated by applying (4). It is assumed that the modulus of elasticity varies

continuously throughout the cross-section of the *i*-th layer according to the following hyperbolic law:

$$E_i = \frac{E_{fi}}{2}\left[\frac{1}{1+q_i\dfrac{\dfrac{b}{2}+y_1}{b}}+\frac{1}{1+r_i\dfrac{z_1-z_{1i}}{z_{1i+1}-z_{1i}}}\right] \tag{19}$$

where

$$-\frac{b}{2}\le y_1\le\frac{b}{2} \tag{20}$$

$$z_{1i}\le z_i\le z_{1i+1} \tag{21}$$

In (19), E_{fi} is the value of the modulus of elasticity in the upper left-hand vertex of the *i*-th layer cross-section, q_i and r_i are material properties which control the material inhomogeneity, respectively, in width and thickness direction of the layer, z_{1i} and z_{1i+1} are the coordinates, respectively, of the upper and lower surfaces of the *i*-th layer in the lower crack arm (Fig. 5).

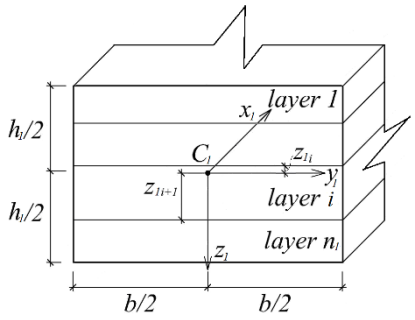

Figire 5. Cross-section of the lower crack arm of the four-point bending multilayered beam

By substituting (19) in equations (10) – (15), one obtains the following expression:

$$\varepsilon_{C_1}+\kappa_{Z_1}z_{1ai}=\frac{\nu_{1i}}{E_{fi_i}\psi_i}+\frac{\nu_{1i}^{\frac{1}{m_i}}}{H_i^{\frac{1}{m_i}}} \tag{22}$$

$$\kappa_{y_1}E_{fi}\psi_i-2\varepsilon_{C_1}\frac{E_{fi}q_i}{b\left(2+q_i\right)^2}=\nu_{2i}+$$
$$+\frac{1}{H_i^{\frac{1}{m_i}}}\left(\begin{array}{l}-2\dfrac{E_{fi}q_i}{b\left(2+q_i\right)^2}\nu_{1i}^{\frac{1}{m_i}}+\\ +E_{fi}\psi_i\dfrac{1}{m_i}\nu_{1i}^{\frac{1-m_i}{m_i}}\nu_{2i}\end{array}\right) \tag{23}$$

$$\kappa_{z_1}E_{fi}\psi_i-\varepsilon_{C_1}\frac{E_{fi}r_i\zeta_i}{2\theta_i^2}=\nu_{3i}+$$
$$\frac{1}{H_i^{\frac{1}{m_i}}}\left(-\frac{E_{fi}r_i\zeta_i}{2\theta_i^2}\nu_{1i}^{\frac{1}{m_i}}+E_{fi}\psi_i\frac{1}{m_i}\nu_{1i}^{\frac{1-m_i}{m_i}}\nu_{3i}\right) \tag{24}$$

$$\begin{aligned}&-4\kappa_{y_1}\frac{E_{fi}q_i}{b\left(2+q_i\right)^2}+\varepsilon_{C_1}\frac{8E_{fi}q_i^2}{b^2\left(2+q_i\right)^3}=\\&=2\nu_{4i}+\frac{1}{H_i^{\frac{1}{m_i}}}\left[\frac{8E_{fi}q_i^2}{b^2\left(2+q_i\right)^3}\nu_{1i}^{\frac{1}{m_i}}-\right.\\&-\frac{2E_{fi}q_i}{b\left(2+q_i\right)}\frac{1}{m_i}\nu_{1i}^{\frac{1-m_i}{m_i}}\nu_{2i}+\\&+\left(-\frac{2E_{fi}q_i}{b\left(2+q_i\right)^2}\frac{1}{m_i}\nu_{1i}^{\frac{1-m_i}{m_i}}+\right.\\&\left.\left.+E_{fi}\psi_i\frac{1-m_i}{m_i^2}\nu_{1i}^{\frac{1-2m_i}{m_i}}\nu_{2i}\right)\nu_{2i}+\right.\\&\left.+E_{fi}\psi_i\frac{2}{m_i}\nu_{i1}^{\frac{1-m_i}{m_i}}\nu_{4i}\right]\end{aligned} \tag{25}$$

$$-\kappa_{y_1}\frac{E_{fi}r_i\zeta_i}{2\theta_i^2}-\kappa_{z_1}\frac{2E_{fi}q_i}{b\left(2+q_i\right)^2}=$$

$$=\nu_{5i}+\frac{1}{H_i^{\frac{1}{m_i}}}\Big[-\frac{2E_{fi}q_i}{b\left(2+q_i\right)^2}\frac{1}{m_i}\nu_{1i}^{\frac{1-m_i}{m_i}}\nu_{3i}+$$

$$+\Big(-\frac{E_{fi}r_i\zeta_i}{2\theta_i^2}\frac{1}{m_i}\nu_{i1}^{\frac{1-m_i}{m_i}}+ \tag{26}$$

$$+E_{fi}\psi_i\frac{1-m_i}{m_i^2}\nu_{1i}^{\frac{1-2m_i}{m_i}}\nu_{3i}\Big)\nu_{2i}+$$

$$+E_{fi}\psi_i\frac{1}{m_i}\nu_{1i}^{\frac{1-m_i}{m_i}}\nu_{5i}\Big]$$

$$-2\kappa_{z_1}\frac{E_{fi}r_i\zeta_i}{2\theta_i^2}+\varepsilon_{C_1}\frac{E_{fi}r_i^2\zeta_i}{\theta_i^3}=$$

$$=2\nu_{6i}+\frac{1}{H_i^{\frac{1}{m_i}}}\Bigg[\frac{E_{fi}r_i^2\zeta_i}{\theta_i^3}\nu_{1i}^{\frac{1}{m_i}}-$$

$$-\frac{E_{fi}r_i\zeta_i}{2\theta_i^2}\frac{1}{m_i}\nu_{1i}^{\frac{1-m_i}{m_i}}\nu_{3i}+\Big(-\frac{E_{fi}r_i\zeta_i}{2\theta_i^2}\frac{1}{m_i}\nu_{1i}^{\frac{1-m_i}{m_i}} \tag{27}$$

$$+E_{fi}\psi_i\frac{1-m_i}{m_i^2}\nu_{1i}^{\frac{1-2m_i}{m_i}}\nu_{3i}\Big)\nu_{3i}$$

$$+E_{fi}\psi_i\frac{2}{m_i}\nu_{1i}^{\frac{1-m_i}{m_i}}\nu_{6i}\Big]$$

where

$$\psi_i=\frac{1}{2}\left[\frac{2}{2+q_i}+\frac{z_{1i+1}-z_{1i}}{z_{1i+1}-z_{1i}+r_i\left(z_{1ai}-z_{1i}\right)}\right] \tag{28}$$

$$\zeta_i=z_{1i+1}-z_{1i} \tag{29}$$

$$\theta_i=z_{1i+1}-z_{1i}+r_i\left(z_{1ai}-z_{1i}\right) \tag{30}$$

Further, by substituting of (7) in equations (16) – (18), one obtains

$$N_1=b\left(z_{1i+1}-z_{1i}\right)\left(\nu_{1i}+\nu_{4i}\frac{b^2}{12}\right)+$$

$$+\frac{1}{2}\nu_{3i}b\left[\left(z_{1i+1}-z_{1ai}\right)^2-\left(z_{1i}-z_{1ai}\right)^2\right]+ \tag{31}$$

$$+\frac{1}{3}\nu_{6i}b\left[\left(z_{1i+1}-z_{1ai}\right)^3-\left(z_{1i}-z_{1ai}\right)^3\right]$$

$$M_{y_1}=\frac{b}{2}\left(z_{1i+1}^2-z_{1i}^2\right)\left(\nu_{1i}-\nu_{3i}z_{1ai}+\right.$$

$$\left.+\nu_{4i}\frac{b^2}{12}+\nu_{6i}z_{1ai}^2\right)+\frac{1}{3}\left(z_{1i+1}^3-z_{1i}^3\right) \tag{32}$$

$$\left(\nu_{3i}b-2\nu_{6i}bz_{1ai}\right)+\frac{1}{4}\nu_{6i}b\left(z_{1i+1}^4-z_{1i}^4\right)$$

$$M_{z_1}=\frac{b^3}{12}\nu_{2i}\left(z_{1i+1}-z_{1i}\right)+$$

$$+\frac{b^3}{24}\nu_{5i}\left[\left(z_{1i+1}-z_{1ai}\right)^2-\left(z_{1i}-z_{1ai}\right)^2\right] \tag{33}$$

where (Fig. 4)

$$N_1=0 \tag{34}$$

$$M_{y_1}=Fl_1 \tag{35}$$

$$M_{z_1}=0 \tag{36}$$

In formulas (22) – (33), $i=1,2,...,n_1$.

Equations (22) – (27) and (31) – (33) should be solved with respect to ε_{C_1}, κ_{y_1}, κ_{z_1}, ν_{1i}, ν_{2i}, ν_{3i}, ν_{4i}, ν_{5i} and ν_{6i} by using the MATLAB computer program. Then, u_{01i}^* is obtained by substituting of (7) in (4).

Since the upper crack arm is free of stresses,

$$u_{02i}^*=0,\ i=1,2,...,n_2. \tag{37}$$

Formula (4) is applied also to calculate the complementary strain energy densities in the layers of the beam cross-section ahead of the crack front. For this purpose, ε_{C_1}, κ_{y_1}, κ_{z_1}, ν_{1i}, ν_{2i}, ν_{3i}, ν_{4i}, ν_{5i}, ν_{6i}, n_1, z_{1i}, z_{1i+1}, N_1, M_{y_1} and M_{z_1} are replaced, respectively, with ε_{C_3}, κ_{y_3}, κ_{z_3}, ν_{r1i}, ν_{r2i}, ν_{r3i}, ν_{r4i}, ν_{r5i}, ν_{r6i}, n, z_{3i}, z_{3i+1}, N_3, M_{y_3} and M_{z_3} in equations (22) – (27) and (31) – (33)

where z_{3i} and z_{3i+1} are the coordinates, respectively, of the upper and lower surfaces of the *i*-th layer in the beam cross-section ahead of the crack front. Then, after solving of equations (22) – (27) and (31) – (33) with respect to ε_{C_3}, κ_{y_3}, κ_{z_3}, ν_{r1i}, ν_{r2i}, ν_{r3i}, ν_{r4i}, ν_{r5i} and ν_{r6i}, the stress, σ_{ri}, is expressed by replacing of ν_{1i}, ν_{2i}, ν_{3i}, ν_{4i}, ν_{5i}, ν_{6i}, z_1, y_1 and z_{1ai}, respectively, with ν_{r1i}, ν_{r2i}, ν_{r3i}, ν_{r4i}, ν_{r5i}, ν_{r6i}, z_3, y_3 and z_{3ai} in (7) (z_{3ai} is calculated by replacing of z_{1i} and z_{1i+1}, respectively, with z_{3i} and z_{3i+1} in (6)). The complementary strain energy density is determined by substituting of σ_{ri} in (4).

After replacing of b_S with b and substituting of u_{01i}^*, u_{02i}^* and u_{0i}^* in (3), the strain energy release rate, obtained by integrating of (3) with help of the MATLAB computer program, is doubled in view of the symmetry (Fig. 4).

In order to verify the solution to the strain energy release rate, the delamination fracture behaviour of the multilayered beam (Fig. 4) is analyzed also by using the method of *J*-integral [20]. The integration is carried-out along the integration contour, Γ, (Fig. 4). Since the upper crack arm is free of stresses, the *J*-integral value is zero in the upper crack arm. Therefore, the *J*-integral solution is written as

$$J = 2(J_{\Gamma_1} + J_{\Gamma_2}) \tag{38}$$

where J_{Γ_1} and J_{Γ_2} are, respectively, the *J*-integral solutions in segments, Γ_1 and Γ_2, of the integration contour. The segments, Γ_1 and Γ_2, coincide, respectively, with the cross-sections of the lower crack arm and the beam ahead of the crack front (Fig. 4). The term in brackets in (38) is doubled in view of symmetry (Fig. 4).

In segment, Γ_1, of the integration contour, the *J*-integral is written as

$$J_{\Gamma_1} = \sum_{i=1}^{i=n_1} \int_{z_{1i}}^{z_{1i+1}} \left[u_{01i} \cos\alpha_{\Gamma_1} - \left(p_{x_i} \frac{\partial u}{\partial x} + p_{y_i} \frac{\partial v}{\partial x} \right) \right] ds \tag{39}$$

where u_{01i} is the strain energy density in the *i*-th layer of lower crack arm behind the crack front, α_{Γ_1} is the angle between the outwards normal vector to the contour of integration and the crack direction, p_{x_i} and p_{y_i} are the components of the stress vector, *u* and *v* are the components of the displacement vector with respect to the coordinate system *xy*, and *ds* is a differential element along the contour of integration. The components of (39) are determined as

$$p_{x_i} = -\sigma_i \tag{40}$$

$$p_{y_i} = 0 \tag{41}$$

$$ds = dz_1 \tag{42}$$

$$\cos\alpha_{\Gamma_1} = -1 \tag{43}$$

$$\frac{\partial u}{\partial x} = \varepsilon = \varepsilon_{C_1} + \kappa_{y_1} y_1 + \kappa_{z_1} z_1 \tag{44}$$

The strain energy density in the *i*-th layer of the lower crack arm is calculated by the formula [19]

$$u_{01i} = \frac{\sigma_i^2}{2E_i} + \frac{\sigma_i^{\frac{1+m_i}{m_i}}}{(1+m_i) H^{\frac{1}{m_i}}} \tag{45}$$

In formulae (40) and (45), the normal stress, σ_i, is determined by (7).

The *J*-integral in segment, Γ_2, is expressed as

$$J_{\Gamma_2} = \sum_{i=1}^{i=n} \int_{z_{3i}}^{z_{3i+1}} \left[u_{0i} \cos\alpha_{\Gamma_2} - \left(p_{xr_i} \frac{\partial u}{\partial x_r} + p_{yr_i} \frac{\partial v}{\partial x_r} \right) \right] ds_r \tag{46}$$

where

$$p_{xr_i} = \sigma_{ri} \tag{47}$$

$$p_{yr_i} = 0 \tag{48}$$

$$ds_r = -dz_3 \tag{49}$$

$$\cos\alpha_{\Gamma_2} = 1 \tag{50}$$

$$\frac{\partial u}{\partial x_r} = \varepsilon_{C_3} + \kappa_{y_3} y_3 + \kappa_{z_3} z_3 \tag{51}$$

$$u_{0i} = \frac{\sigma_{ri}^2}{2E_i} + \frac{\sigma_{ri}^{\frac{1+m_i}{m_i}}}{\left(1+m_i\right) H^{\frac{1}{m_i}}} \tag{52}$$

The average value of the *J*-integral along the delamination crack front is written as

$$J_{av} = \frac{1}{b} \int_{-\frac{b}{2}}^{\frac{b}{2}} J\, dy_1 \tag{53}$$

By substituting of (39) and (46) in (53), one arrives at

$$J = \frac{2}{b} \sum_{i=1}^{i=n_1} \int_{-\frac{b}{2}}^{\frac{b}{2}} \int_{z_{1i}}^{z_{1i+1}} \left[u_{01i} \cos\alpha_{\Gamma_1} - \left(p_{x_i} \frac{\partial u}{\partial x} + p_{y_i} \frac{\partial v}{\partial x} \right) \right] ds dy_1 + \\ + \frac{2}{b} \sum_{i=1}^{i=n} \int_{-\frac{b}{2}}^{\frac{b}{2}} \int_{z_{3i}}^{z_{3i+1}} \left[u_{0i} \cos\alpha_{\Gamma_2} - \left(p_{xr_i} \frac{\partial u}{\partial x_r} + p_{yr_i} \frac{\partial v}{\partial x_r} \right) \right] ds_r dy_1 \tag{54}$$

The integration in (54) should be performed by the MATLAB computer program. The fact that the *J*-integral values obtained by (54) exactly match the strain energy release rates calculated by (3) conforms the correctness of the delamination fracture analysis developed in the present paper. It should be mentioned that the delamination is analyzed also by keeping more than six members in the series of Taylor (5). The results are very close to these obtained by keeping the first six members (the difference is less than 3 %).

Effects of the material inhomogeneity and the non-linear mechanical behaviour of the material on the delamination fracture are evaluated. For this purpose, calculations are carried-out by applying the solution to the strain energy release rate (3). The results obtained are presented in non-dimensional form by using the formula $G_N = G / \left(E_{f1} b \right)$. In order to elucidate the influence of the delamination crack location along the beam height, two three-layered four-point bending beam configurations are

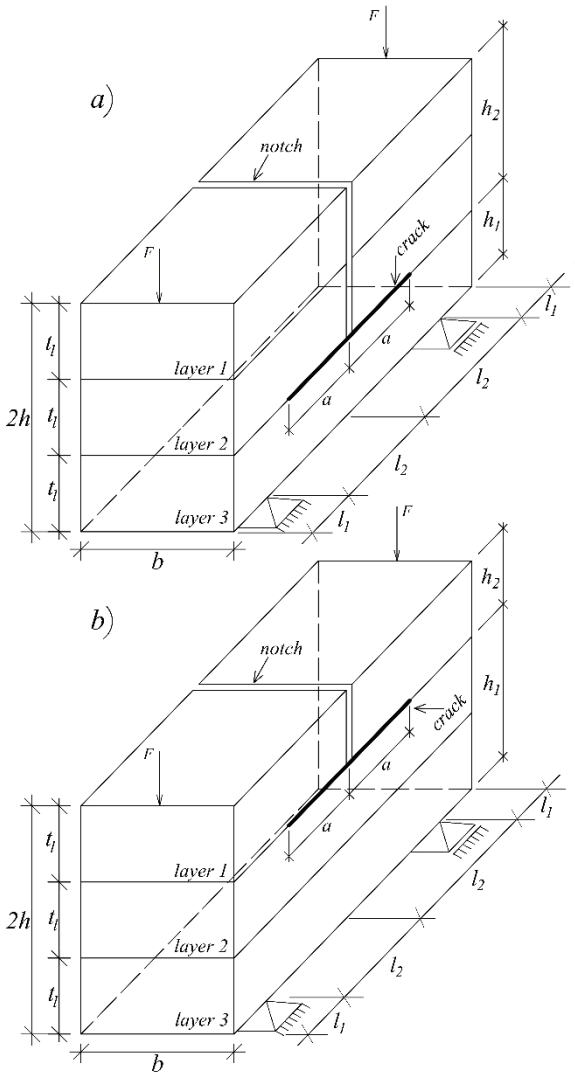

Figure 6. Two three-layered four-point bending beam configurations with delamination crack located between (a) layers 2 and 3, and (b) layers 1 and 2

investigated (Fig. 6). In the first configuration, the delamination crack is located between layers 2 and 3 (Fig. 6a). A delamination crack between layers 1 and 2 is analyzed in the beam configuration shown in Fig. 6b. The thickness of each layer in both configurations is t_l. It is determined that $b = 0.025$ m, $t_l = 0.006$ m, $l_1 = 0.060$ m, $l_2 = 0.100$ m and $F = 10$ N. The material inhomogeneity in width and thickness direction of layers is characterized by q_i and r_i.

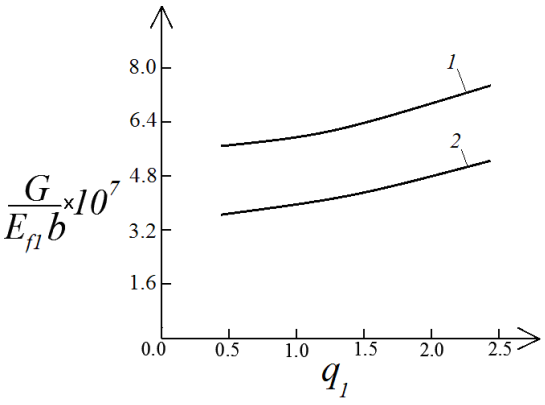

Figure 7. The strain energy release rate in non-dimensional form presented as a function of q_1 for three-layered four-point bending beam configuration with delamination crack located (curve 1) between layers 2 and 3, and (curve 2) between layers 1 and 2 (refer to Fig. 6)

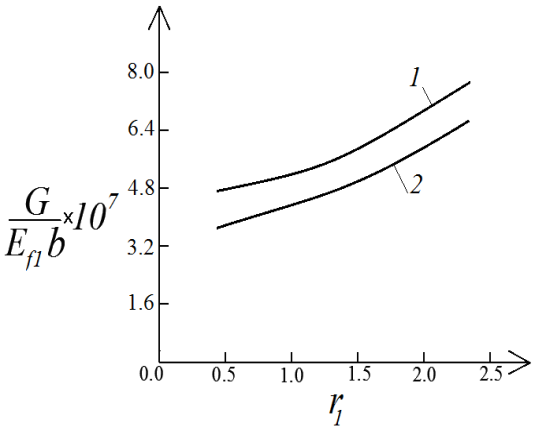

Figure 8. The strain energy release rate in non-dimensional form presented as a function r_1 at (curve 1) non-linear mechanical behavior of the material and (curve 2) linear-elastic behaviour of the material for the three-layered four-point bending beam configuration with delamination crack located between layers 2 and 3 (refer to Fig. 6a)

In order to elucidate the influence of q_1 on the delamination fracture behavior, the strain energy release rate in non-dimensional form is presented as a function of q_1 in Fig. 7 for both three-layered beam configurations assuming that $E_{f2}/E_{f1}=0.6$, $E_{f3}/E_{f1}=0.8$, $H_1/E_{f1}=0.7$, $H_2/H_1=1.4$, $H_3/H_1=0.5$, $m_1=m_2=m_3=0.8$, $q_2=0.6$, $q_3=1.4$, $r_1=2.5$, $r_2=1.5$ and $r_3=1.8$. One can observe in Fig. 7 that the strain energy release rate increases with increasing of q_1. This behaviour is attributed to the fact that the beam stiffness increases with increasing of q_1. The curves in Fig. 7 indicate also that the strain energy release rate is lower when the delamination crack is located between layers 1 and 2 (Fig. 6b). This finding is explained with the fact that the thickness of the lower crack arm is higher when the delamination crack is between layers 1 and 2.

The effect of r_1 on the delamination fracture behaviour is shown in Fig. 8 where the strain energy release rate is presented in non-dimensional form as a function of r_1 at $q_1=2.2$.

The three-layered beam configuration shown in Fig. 6a is investigated. It can be observed in Fig. 8 that that strain energy release rate increases with increasing of r_1. The effect of the non-linear mechanical behaviour of the material on the delamination fracture behaviour is elucidated too.

For this purpose, the strain energy release rate is presented in Fig. 8 that is obtained assuming linear-elastic behaviour of the inhomogeneous material in each layer of the beam configuration in non-dimensional for comparison with the non-linear solution. It should be mentioned that the linear-elastic solution to the strain energy release rate is derived by substituting of $H\to\infty$ in the non-linear solution (3) since at $H\to\infty$ the Ramberg-Osgood stress-strain relation (1) transforms in the Hooke's law assuming that E_i is the modulus of elasticity of the inhomogeneous material in the *i*-th layer of the beam. The curves in Fig. 8 show that the non-linear mechanical behaviour of the material leads to increase of the strain energy release rate.

4 Conclusions

Delamination fracture behaviour of multilayered non-linear elastic beam structures has been investigated in this paper assuming that each layer exhibits smooth material inhomogeneity along the width as well as along thickness of the layer. The Ramberg-Osgood stress-strain relation is used for treating the non-linear mechanical behaviour of the

inhomogeneous material. The delamination fracture behaviour is studied assuming that the modulus of elasticity varies continuously in the cross-section of each layer. A general approach for analysis of the strain energy release rate for delamination cracks in multilayered non-linear elastic inhomogeneous beams is developed in contrast to the previously published papers which consider particular multilayered beam configurations [15, 17]. The approach holds for beams of arbitrary cross-section in contrast to the previous papers which consider beams of rectangular cross-section. The approach can be applied at arbitrary distribution of the modulus of elasticity in both width and thickness directions of each layer of the beam (the previous papers consider particular distributions). The approach is valid for beams made of arbitrary number of layers. Each layer has individual thickness and material properties. The delamination crack is located arbitrary along the height of the multilayered beam. Besides, the approach can be used also when the law for distribution of the modulus of elasticity is different in each layer in contrast to the previous papers which are based on the assumption that the law is the same in each layer [15, 17]. It should be noted that the approach holds for non-linear elastic behaviour of the material. However, the approach can be applied also for elastic-plastic behaviour if the beam undergoes active deformation, i.e. if the external load increases only.

The general approach is applied for studying the delamination fracture behaviour of a multilayered beam configuration of rectangular cross-section. The beam is subjected to four-point bending. A delamination crack is located symmetrically with respect to the beam mid-span. The strain energy release rate is determined assuming that the continuous variation of the modulus of elasticity in the cross-section of each layer is described by a hyperbolic law. The delamination fracture behaviour is studied also by applying the *J*-integral method for verification of the solution to the strain energy release rate. Effects of material inhomogeneity in width and thickness directions of the layer, the delamination crack location along the beam height and the non-linear mechanical behaviour of the inhomogeneous material on the delamination fracture behaviour are elucidated. The analysis reveals that the strain energy release rate increases with increasing of q_1 and r_1. This finding is attributed to a decrease of the beam stiffness with increasing of q_1 and r_1. It is also found that the strain energy release rate decreases with increasing of the lower crack arm height. Concerning the effect of the non-linear mechanical behavior of the inhomogeneous material on the delamination fracture, the investigation shows that the strain energy release rate increases when the material non-linearity is taken into account in the fracture analysis. The topic can be studied further in the future by assuming that not only the modulus of elasticity but also the other material properties, H_i and m_i, vary continuously in the cross-section of each layer of the beam. Also, the approach can be sophisticated further by considering the rheological behaviour (creep of strains and relaxation of stresses) and its influence on the delamination.

References

[1] Xing, A., Jun, Z., Chuanzhen, H., Jianhua, Z.: *Development of an advanced ceramic tool material – functionally gradient cutting ceramics.* Mater. Sci. Eng., A 248(1998), 125-131.

[2] Lu, C.F., Lim, C.W., Chen, W.Q.: *Semi-analytical analysis for multi-dimensional functionally graded plates: 3-D elasticity solutions*, Int. J. Num. Meth. Engineering, 79(2009), 3, 25-44.

[3] Markworth, A.J., Ramesh, K.S., Parks, Jr.W.P.: *Review: modeling studies applied to functionally graded materials*, J. Mater. Sci., 30(1995), 3, 2183-2193.

[4] Nemat-Allal, M.M., Ata, M.H., Bayoumi, M.R. Khair-Eldeen, W.: *Powder metallurgical fabrication and microstructural investigations of Aluminum/Steel functionally graded material*, Materials Sciences and Applications, 2(2011), 2, 1708-1718.

[5] Gasik, M.M.: *Functionally graded materials: bulk processing techniques*, International Journal of Materials and Product Technology, 39(2010), 4, 20-29.

[6] Butcher, R.J., Rousseau, C.E., Tippur, H.V.: *A functionally graded particulate composite: Measurements and Faiure Analysis*, Acta Matererialia, 47(1999), 1, 259-268.

[7] Bykov, Yu.V., Egorov, S.V., Ermeev, A.G., Holoptsev, V.V.: *Fabrication of metal-ceramic functionally graded materials by microwave sintering*, Inorganic Materials: Applied Research 3(2012), 3, doi: 10.1134/S207511 33120300057.

[8] Lu, C.F., Lim, C.W., Chen, W.Q.: *Semi-analytical analysis for multi-dimensional functionally graded plates: 3-D elasticity solutions*, Int. J. Num. Meth. Engng, 79(2009), 5, 25-44.
[9] Koizumi, M.: *The concept of FGM Ceramic Trans*., Functionally Gradient Materials, 34(1993), 3, 3-10.
[10] Suresh, S., Mortensen, A.: *Fundamentals of functionally graded materials*. IOM Communications Ltd, London, 1998.
[11] Prasad, P.: *Design and Analysis of a Disc Brake by Using Functional Graded Materials*, International Journal of Research, 4(2017), 6, 103-110.
[12] Bohidar, S.K., Sharma, R., Mishra, P.R.: *Functionally graded materials: A critical review*, International Journal of Research, 1(2014), 4, 289-301.
[13] Dolgov, N. A.: *Determination of Stresses in a Two-Layer Coating*, Strength of Materials, 37(2005), 4, 422-431.
[14] Dolgov, N. A.: *Analytical Methods to Determine the Stress State in the Substrate–Coating System Under Mechanical Loads*, Strength of Materials, 48(2016), 5, 658-667.
[15] Rizov, V.: *Analytical study of delamination in multilayered two-dimensional functionally graded non-linear elastic beams*, Journal of Mechanics, (2017), DOI:10.1017/jmech.2017. 104.
[16] Rizov, V.I.: F*racture analysis of functionally graded beams with considering material non-linearity*, Structural Engineering and Mechanics, 64(2017), 4, 487-494.
[17] Rizov, V.I.: *Delamination of Multilayered Functionally Graded Beams with Material Nonlinearity*, International Journal of Structural Stability and Dynamics, (2018), doi.org/10.1142/S0219455418500517.
[18] Rizov, V.: *An analytical solution to the strain energy release rate of a crack in functionally graded beams*, European journal of mechanics A/solids, 65(2017), 6, 301-312.
[19] Rizov, V.: *Lengthwise fracture analyses of functionally graded beams by the Ramberg-Osgood equation*, Engineering Review, 38(2018), 3, 309-320.
[20] Broek, D.: *Elementary engineering fracture mechanics*. Springer, 1986.